Materials Today: Proceedings 72 (2023) 1725–1734

Contents lists available at ScienceDirect

Materials Today: Proceedings

journal homepage: www.elsevier.com/locate/matpr

Analysis for effect of optimized air drag braking system on the drag force of vehicle

Pravin Hujare [a,*], Ashwin Shelke [a], Hrunil Kansepatil [a], Dinesh Kamble [a], Deepak Hujare [b], Umesh Chavan [c]

[a] Mechanical Engineering Department, Vishwakarma Institute of Information Technology, Pune 48, India
[b] School of Mechanical Engineering , MIT World Peace University, Pune 38, India
[c] Mechanical Engineering Department, Vishwakarma Institute of Technology, Pune 37, India

ARTICLE INFO

Article history:
Available online 5 October 2022

Keywords:
Air drag braking system
Coefficient of drag
Drag force
Taguchi optimization
CFD analysis

ABSTRACT

The drag force acting on the vehicle has a significant role in the braking efficiency of the vehicle. The braking efficiency is directly proportional to the drag force acting on vehicle. Using add-on gadgets on the vehicle, the drag force can be enhanced. This paper deals with the effect of an additional air drag braking system on drag force of a passenger car. The drag force and drag coefficient of a passenger car is estimated by using Computational Fluid Dynamics (CFD) analysis. An increase in the drag force is observed to the attachment of an additional air drag braking system. In order to optimize the dimensions of the drag braking system for the highest drag force, Taguchi Optimisation is performed. It is found that optimized drag braking system improves the braking efficiency of passenger car. The experimental analysis is performed on a clay model of a passenger car with reduced scale 1:16 in a wind tunnel. It is found that the amount of braking effort is reduced significantly due to the application of this new concept, air drag braking system. The numerical analysis results appear to be in good agreement with those from experimental analysis.

Selection and peer-review under responsibility of the scientific committee of the 2nd International Conference and Exposition on Advances in Mechanical Engineering.

1. Introduction

When a vehicle moves on a road, it is subjected to various types of forces, including rolling resistance, gravity, acceleration, and aerodynamic drag resistance. The aerodynamic drag resistance becomes increasingly dominant among all resistances as the vehicle speed increases. At high velocities, the ratio of the engine's power output to the body's drag has a more significant influence on the vehicle performance than the specific power (power to weight ratio), which is critical at lower speeds since drag isn't major. Thus, combining the drag and braking force the vehicle will achieve greater braking efficiency and will decelerate rapidly compared to the normal system [1].

2. Materials and methods

The drag force exerted on a body is determined by its geometry, speed, and the medium in which it is travelling [2]. Drag and lift are the most common forces observed.This can be demonstrated using the fluid mechanics equation [1].

$$F_d = \frac{1}{2} C_d \rho A V^2 \quad (1)$$

where F_d is the drag force, C_d represents the drag coefficient, ρ is the fluid density, V represents the object velocity, and A represents the projected frontal area. In the aerodynamic field, the external flow at the upper side of the body is the greatest aspect to consider. The drag coefficient, C_d, is a non-dimensional quantity that represents how much drag an object experiences as a result of airflow [3].

3. Numerical analysis

The numerical analysis of the car model is performed in ANSYS software. For numerical analysis initially CAD model is prepared in Solidworks software. Further this model is then imported into the ANSYS Fluent software for CFD analysis.

* Corresponding author.
E-mail address: pravin.hujare@viit.ac.in (P. Hujare).

https://doi.org/10.1016/j.matpr.2022.09.475
2214-7853/
Selection and peer-review under responsibility of the scientific committee of the 2nd International Conference and Exposition on Advances in Mechanical Engineering.

3.1. Vehicle geometry modelling

A classic Land Rover model was chosen because of the model's simple geometry and shape, in order to get a good sense of the effect of the drag braking system on a real car. Bhavini [4] used a 1:20 reduced scale aluminium car model for his experiments. Due to the size constraints of the wind tunnel, the car under investigation is a 1:16 reduced scale clay model. The full-size car model's dimensions are 4704 mm long, 1800 mm wide, and 1512 mm height.

Due to the significant amount of processing time and power required for such a big model, a 1:16 scale model with dimensions of 294 mm length, 112.5 mm width, and 94.5 mm height was used. The drag braking system is 15.81 mm in length, 91 mm in width, and 14 mm in height. The CAD models of the system are prepared in SOLIDWORKS. Fig. 1 and Fig. 2 depict the CAD model of Car without and with Drag Braking system respectively.

FEA involves the following methodology. Initially a CAD model of Car is designed. Following this, the model is then loaded into the ANSYS Fluent for CFD simulation. A fluid enclosure around it is built in order for simulating the air flow around the vehicle. This enclosure acts as an air domain. The model then proceeds for meshing. In order to more accurately capture the air flow surrounding the vehicle, fine meshing is done close to its surface. Then the appropriate boundary conditions are given to the model. Finally, the results are obtained after the solution convergence criterion is met.

3.2. Mesh generation

Here, initially an automobile's general model has been designed in the Solidworks software followed by, loading the model into ANSYS Fluent to perform the numerical analysis and calculate the drag coefficient in the wind enclosure [5].After much deliberation the tetrahedral type of mesh was chosen for meshing the entire system in this study. Finer mesh is selected for the car surface, in order to catch the flow in the zone nearest to the vehicle as well as in the wake. A size of 1.5 mm is set for the car surface and 11 mm for the air domain. Fig. 3 and Fig. 4 depict the meshing performed for the car model.

3.3. CFD simulation and setup

ANSYS FLUENT software is used to conduct a CFD simulation of the meshed model in order to determine the drag coefficient and drag force, as well as visualise the air flow streamlines and pressure contours at various locations on the vehicle [6]. A tetrahedral surface mesh of the vehicle is generated with a size of 1.5 mm. The enclosure inlet plane was named 'velocity inlet'. The velocity of the air through the inlet was assigned a value of 23 m/s. The enclosure outlet plane is designated as 'pressure outlet,' and the pressure is set to be constant and equal to atmospheric pressure. The backflow turbulence intensity of 10 % and viscosity ratio of 10 were used to create the turbulence for the pressure outlet. Implementing turbulence modelling with conventional k-ε model employing upgraded wall functions and second order upwind discretization method for the Turbulence Kinetic energy, Momentum, and Turbulence Dissipation rate resulted in a Navier-Stokes equation [7]. The procedure is then repeated for the car with drag braking system, and it's respective drag coefficient value is calculated.

For this analysis, certain assumptions are taken into consideration such as outlet pressure constant, vehicle surfaces with no slip wall boundary conditions, inlet having steady state air flow with constant velocity, zero-degree yaw angle and the all sides of the virtual wind tunnel having inviscid flow wall boundary condition [8]. Table 1 gives a summary of the boundary conditions applied.

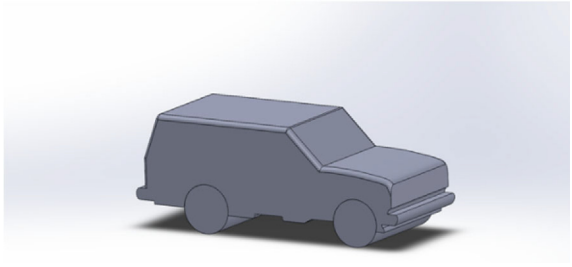

Fig. 1. Vehicle model without Drag Braking system.

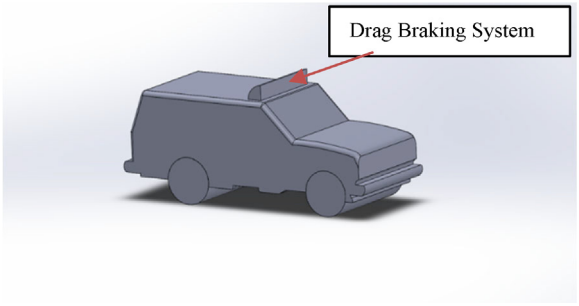

Fig. 2. Vehicle model with Drag Braking system.

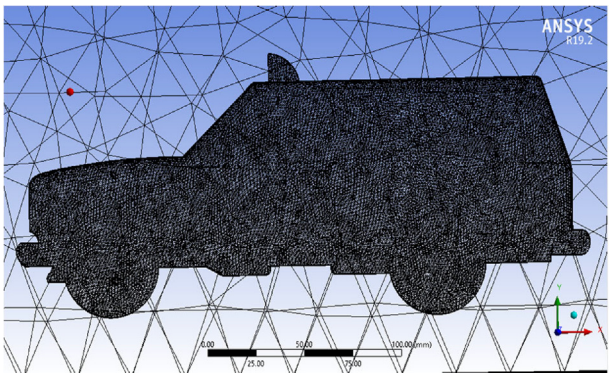

Fig. 3. Meshed Vehicle Surface.

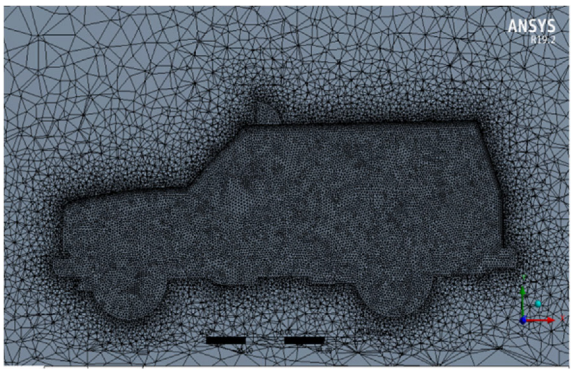

Fig. 4. Section View of Mesh Enclosure.

3.4. Results and discussion

Results of the CFD analysis are obtained in both scenarios, with and without the drag brake system, at a speed of 23 m/s. Also, the

Table 1
Boundary Conditions.

Boundary Conditions		
Velocity Inlet	Magnitude	23 m/s
	Turbulence Specification Method	Intensity and Viscosity Ratio
	Turbulence Intensity	10.00 %
	Turbulence Viscosity Ratio	10
Pressure Outlet	Gauge Pressure magnitude	0
	Gauge Pressure direction	Normal to boundary
Fluid Properties	Fluid Type	Air
	Density	ρ = 1.225 (kg/m^3)

static pressure contours, velocity contours and velocity streamlines are found out. Fig. 5 depicts the Coefficient of Drag (C_d) plot of the baseline model. The C_d value for the car without air drag braking system at the air velocity of 23 m/s was obtained as 0.53307329.

Fig. 6 shows the C_d plot for the car with the air drag braking system. It's C_d value was obtained as 0.78863921. Fig. 7 depicts pressure contours in the car model without Drag Braking system. The colour gradient on the car surface shows the pressure intensity at each particular section of the car, so it's convenient to assess an area of interest. From the Fig. 8, it is observed that a high-pressure region is generated in the frontal section of the car due to the decrease in velocity of air.

Fig. 9 depicts the velocity streamline over the vehicle's surface. The set of curves known as Streamlines are instantaneously tangent to the flow's velocity vector. Thus, it depicts the direction of any fluid element in the enclosure at any point in time.

Fig. 10 and Fig. 11 depict the velocity contours of cars with and without the Drag Braking system respectively. It is observed that due to the Drag Braking system the velocity of the fluid domain near the Drag Braking system is decreased because of the hindrance. This results in an increase of drag force.

In the case of the car with drag braking system, the C_d value is 0.78. The percentage increase in C_d is 47.94 %. Hence Drag force increases proportionally to the Drag Coefficient. Table 2 shows comparison of the Drag Coefficient.

4. Taguchi optimization

Taguchi method is a statistical method of optimizing the critical process parameters for obtaining the best result [9]. In this study, optimal dimensions of the drag braking system for the maximum value of the Drag Coefficient are found out using Taguchi method. The signal-to-noise ratio(S/N), orthogonal array and analysis of variance are used to investigate the variation in the system's drag coefficient values.

4.1. Determining the control factors and their levels

From literature survey, the range for varying the Drag Braking system length is fixed as 15.81 mm to 19.81 mm and for height the range is 14 mm to 18 mm [10]. The control and noise factors are shown in Table 3. The control factors and their levels are shown in Table 4.

4.2. Selection of orthogonal array

For determining the type of orthogonal array to be used, the total degrees of freedom are required to be computed. For a three-level control factor, the degree of freedom is two. Thus, for the two dimensional factors, the degree of freedom is 4. Now while selecting the orthogonal array, the degrees of freedom for an orthogonal array should be at least equal to or greater than those of the control factors. In this study, a L9 orthogonal array was selected for the experiment as shown in Table 5. Therefore, a total of 9 experiments have to be carried out.

4.3. Performing the analysis

In accordance with the above Orthogonal Array, CFD analysis was performed for each combination of the factors as shown in Table 6. Among the noise factors, velocity of medium prominently varies and has a significant effect on the result. Thus, for each set of control factors as shown in Table 7, the analysis was performed for 3 different air velocities of 19, 21, 23 m/s to account for the varia-

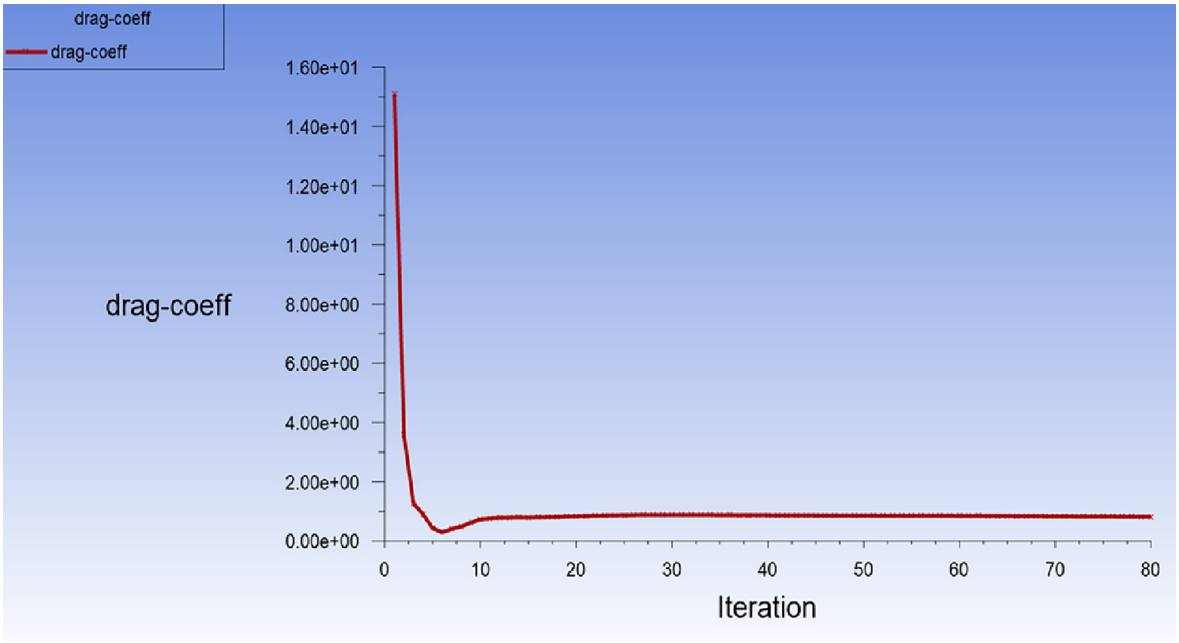

Fig. 5. C_d without Drag Braking system.

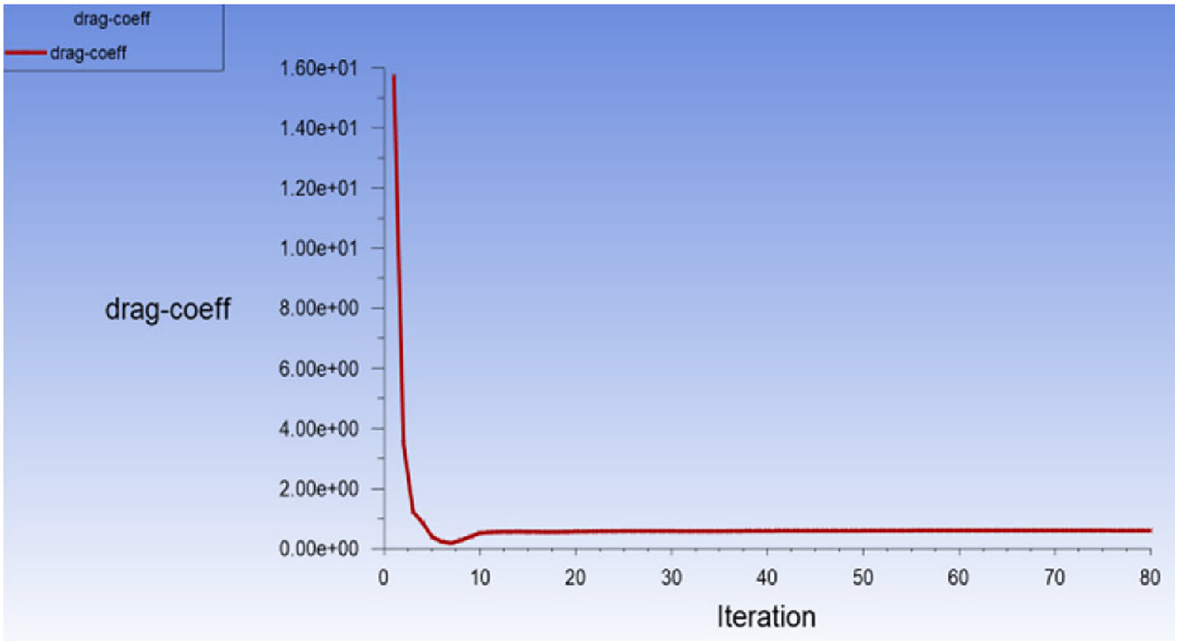

Fig. 6. C_d with Drag Braking System.

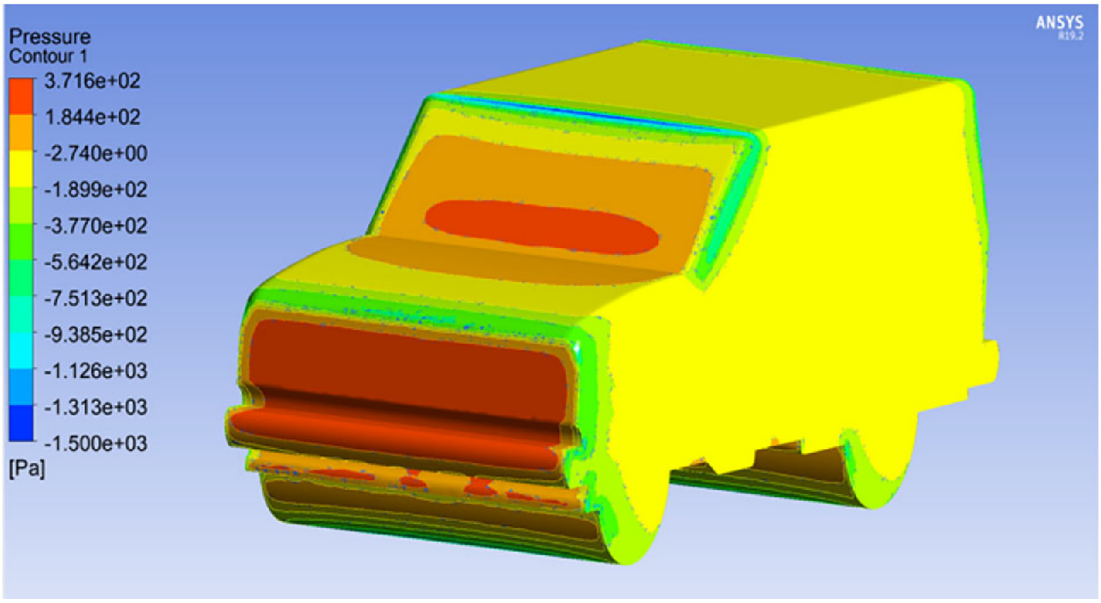

Fig. 7. Pressure contour without Drag Braking system.

tion due to this noise factor.Following this, the Taguchi Optimisation of the objective function (C_d) was performed for the 'larger-the-better' type of control function in statistical analysis software Minitab. The resulting S/N ratio is provided in Table 8, and mean data plots are shown in Fig. 12 as a result.

For the maximum value of C_d, the factors with the highest value of S/N ratio are selected and the resultant value is found for that set. From the plot we can deduce that the S/N ratio is highest for 15.81 mm length and 18 mm height and has a corresponding mean C_d value of 0.892524, the highest among any other. Thus, the most optimum dimensions of the Drag Braking System are found using the Taguchi Optimization method.

5. Experimental analysis

The experimental analysis is performed on clay model of Car. The experimental investigations are performed on car clay model mounted in the wind tunnel [11].

5.1. Experimental setup

Fig. 13 illustrates the schematic diagram of an experimental setup employing a subsonic wind tunnel.

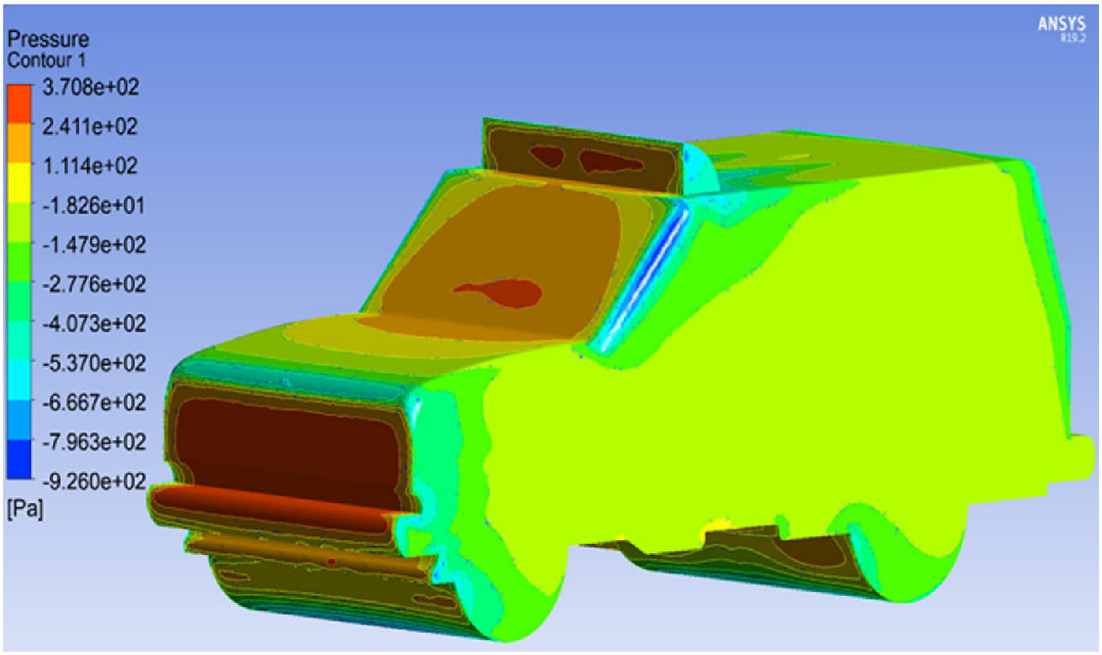

Fig. 8. Pressure contour with Drag Braking system.

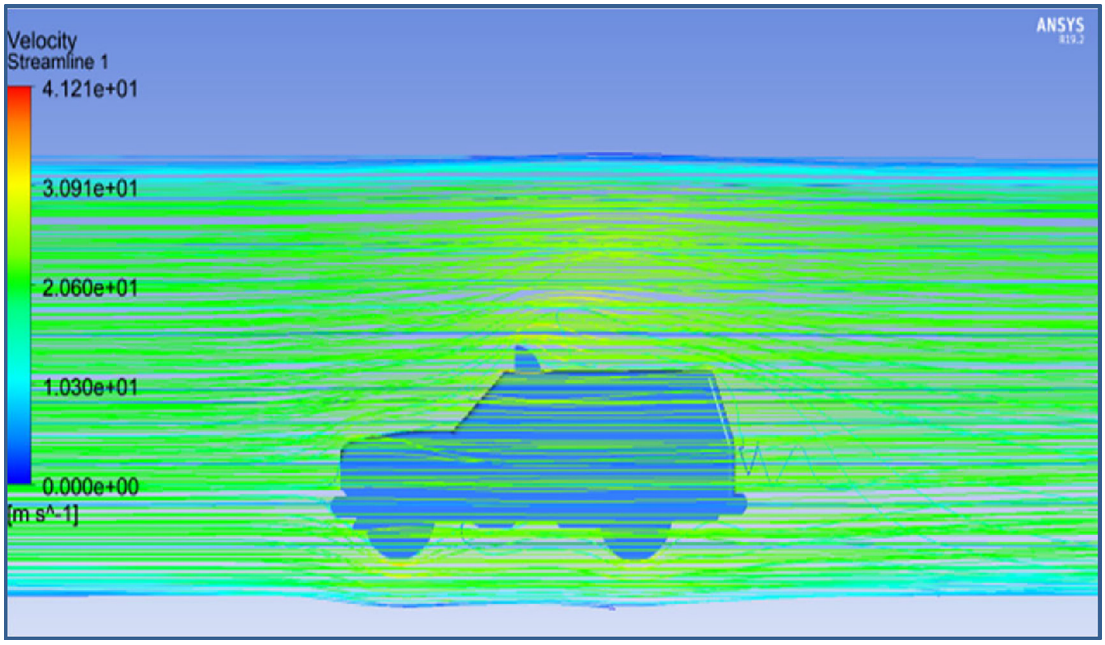

Fig. 9. Velocity Streamline for car with Drag Braking system.

The actual experimental setup is as shown in Fig. 14. It consists of a Honeycomb structure through which air is passed [12]. It is connected to the test section in which the car clay model is placed. The other end of the test section is connected to Diffuser. The pressure difference is measured through a multitude manometer which is connected to Car Clay Model. Using clay modelling tools, a scaled down version (1:16) of the clay model is prepared.

5.2. Experimental procedure

The prepared clay model is now mounted in the experimental setup for testing. The seven different points across the model are considered to take pressure readings. These seven points are connected to multi tube manometer. To identify the locations of the pressure tapping, a separate number is given to each con-

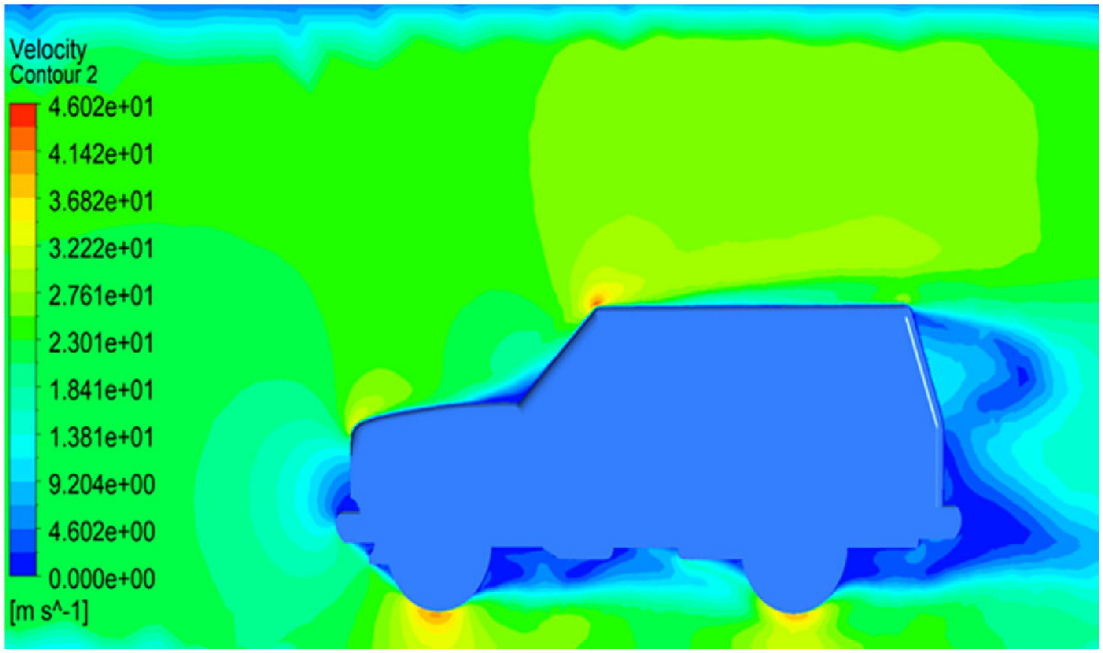

Fig. 10. Velocity Contour without Drag Braking system.

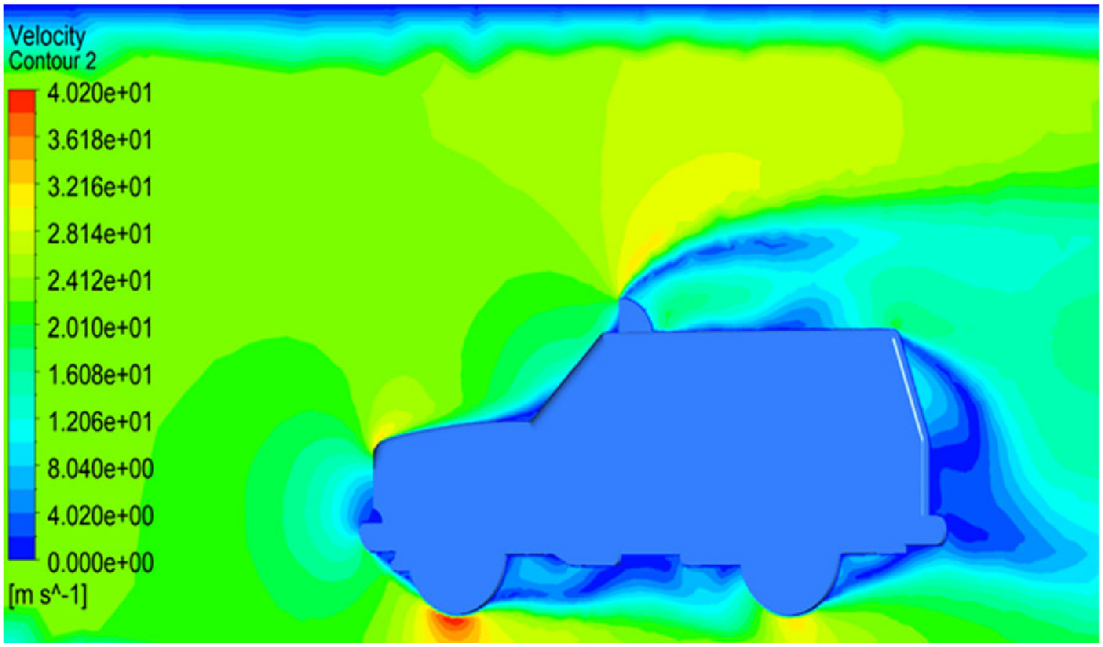

Fig. 11. Velocity Contour with Drag Braking system.

Table 2
Comparison of Drag Coefficient.

Configuration	Drag Coefficient	% Increase in Drag Coefficient from baseline
Baseline car	0.53	0
Car with drag braking system	0.78	47.94

Table 3
Control and Noise Factors.

Control Factors	Noise Factors
Length	Velocity
Height	Air density
	Temperature

Table 4
Control Factors and their Levels.

Factors	Levels		
	1	2	3
Length(mm)	15.81	17.81	19.81
Height(mm)	14	16	18

Table 5
Orthogonal Array.

Expt. No.	Control Factors	
	1	2
1	1	1
2	1	2
3	1	3
4	2	1
5	2	2
6	2	3
7	3	1
8	3	2
9	3	3

Table 6
OA with Control Factors.

Exp No	Length (mm)	Height (mm)
1	15.81	14
2	15.81	16
3	15.81	18
4	17.81	14
5	17.81	16
6	17.81	18
7	19.81	14
8	19.81	16
9	19.81	18

Table 7
Measured Values of C_d at 3 different velocities.

Exp No	Vel_1	Vel_2	Vel_3
1	0.793473	0.791269	0.788639
2	0.887603	0.882652	0.879358
3	0.896448	0.892133	0.888991
4	0.83469	0.830624	0.827077
5	0.819222	0.816441	0.814758
6	0.889983	0.885805	0.883523
7	0.858279	0.854524	0.849985
8	0.872798	0.869115	0.864784
9	0.841731	0.839179	0.836257

Table 8
S/N ratio and Mean Value.

Expt No	S/N ratio	Mean
1	−2.03516	0.791127
2	−1.07897	0.883204
3	−0.98776	0.892524
4	−1.61029	0.830797
5	−1.75768	0.816807
6	−1.04716	0.886437
7	−1.36838	0.854263
8	−1.22080	0.868899
9	−1.52428	0.839055

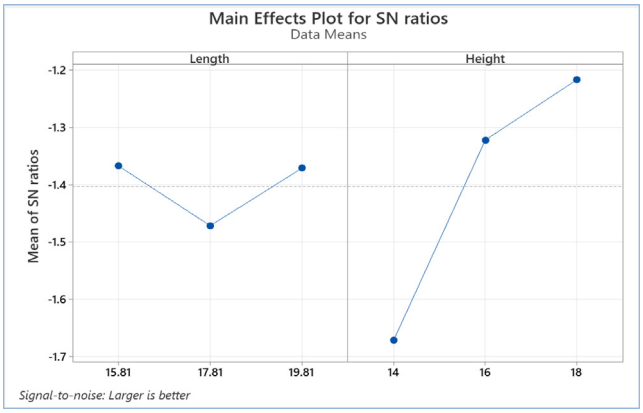

Fig. 12. S/N ratio plot of Length and Height variable.

nection [13]. The Fig. 15 shows the baseline car model used for testing. The Fig. 16 depicts the connection of car model to manometer.

Once the setup is ready, all the connections are re-checked and the experiment is performed. The pressure readings will be taken at different wind velocities and pressure drop across the test section will be calculated which will be used to find the drag coefficient. Powering the wind tunnel on, the speed of wind is regulated by a Knob and shown on the display. For the first reading, the wind speed is brought to and maintained for a while at 10 m/s and indication of the manometer is recorded. The speed is then steadily increased and a manometer reading for each particular velocity is taken. For the experiment, two methods are used: pressure distribution along the centreline and over the entire car profile, and pressure measurement in the effective domain upstream and downstream of the car [14].

The frontal area of the car model used for the experiment is 0.00910234 m^2 and upon attachment of the drag braking system it increases to 0.01043034 m^2. The drag force value is found out for all the velocity values, with and without the drag braking system. Comparing the drag force values between the two cases, it is clear that the model with the air drag braking system generates more drag force than the baseline model and, as a result, achieves higher braking efficiency.

6. Result and discussion

The experiment is carried out in a wind tunnel at different velocities to investigate the impact of the air drag braking system on air drag. Following this, the drag coefficient C_d value is calculated for each of the velocities. The comparisons of experimental and numerical results are shown in Table 9.The experimental examination validates the numerical modelling results with an error of less than 13 %. The experimental setup of the car with the drag braking system is placed in the wind tunnel after the experiment is conducted on the baseline model. In this instance, one additional tube is connected to the braking system for measuring pressure there; bringing the total number of connections to the manometer to 8. Similar to previous experiment, the air velocity in the wind tunnel is increased progressively from 10 m/s to 25 m/s and readings were recorded for ten different velocities at 8 different locations across the car. Following this, the C_d value for this

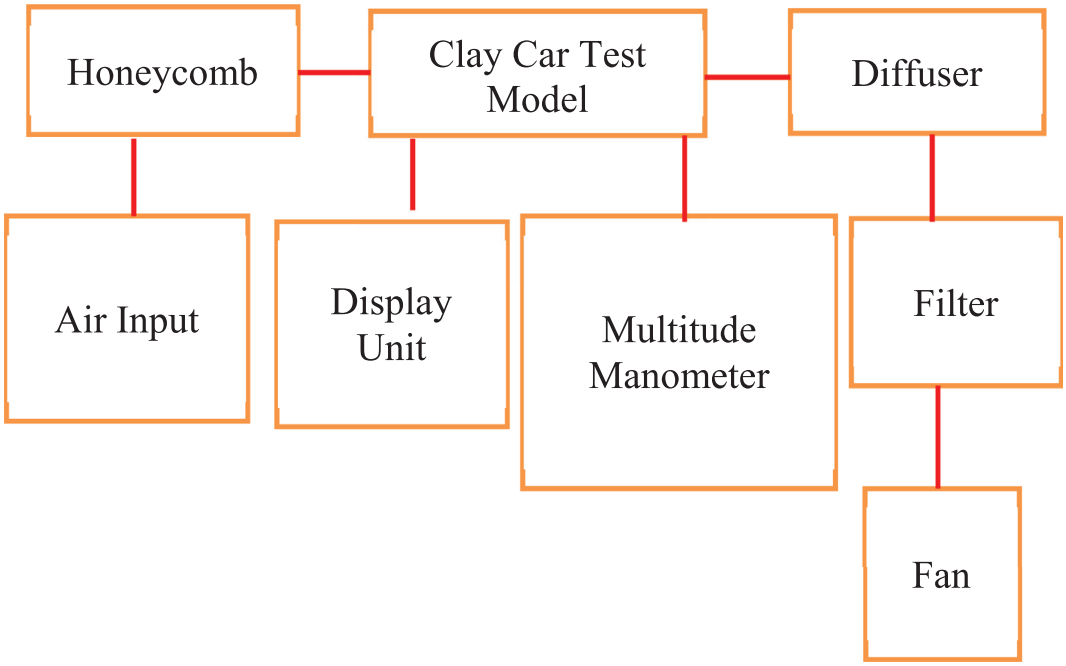

Fig. 13. Schematic diagram of experimental setup.

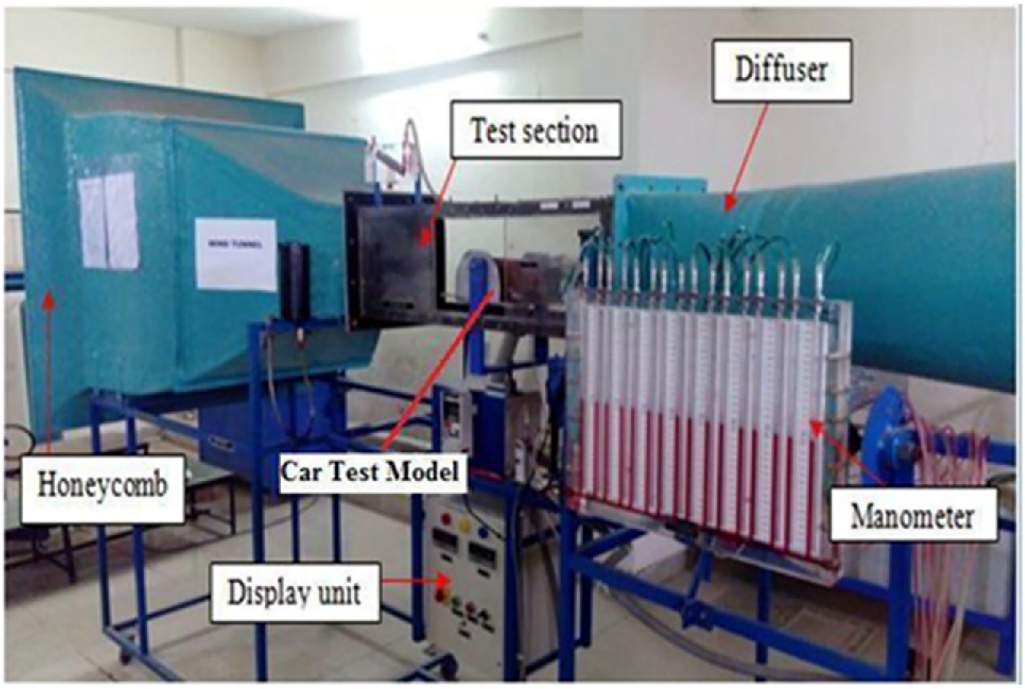

Fig. 14. Actual pictures of experimental setup.

Fig. 15. Experimental car model for test.

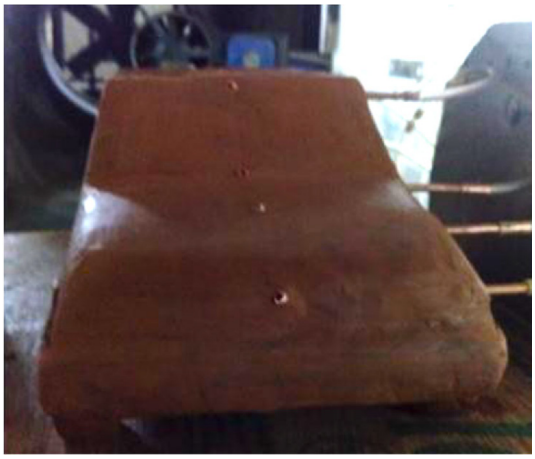

Fig. 16. Car model connected to the manometer.

Table 9
Comparison between numerical and experimental results.

Types of Car System	Numerical	Experimental	% Error
C_d without braking system	0.53307329	0.60121492	12.78
C_d with braking system	0.89252437	0.98568742	10.43

Fig. 17. Car clay model with Drag Braking system.

system is calculated. The Fig. 17 depicts the Car clay model with Drag Braking system used for experimental testing.

The Table 9 shows the comparison of the numerical and experimental results for both of the car systems.

7. Conclusion

The Numerical results appear to be in good agreement with experimental results with a max error of 12.78 %. A 67.44 % increase in drag force is achieved over the baseline model using the Drag Braking technology. It is found that Air Drag Braking system increases the braking efficiency of vehicle.

CRediT authorship contribution statement

Pravin Hujare: Conceptualization, Methodology, Formal analysis, Supervision, Software, Validation, Investigation, Writing – original draft, Writing – review & editing. **Ashwin Shelke:** Conceptualization, Methodology, Formal analysis, Supervision, Software, Validation, Investigation, Writing – original draft, Writing – review & editing. **Hrunil Kansepatil:** Conceptualization, Methodology, Formal analysis, Supervision, Software, Validation, Investigation, Writing – original draft, Writing – review & editing. **Dinesh Kamble:** Software, Validation, Investigation, Writing – original draft, Writing – review & editing. **Deepak Hujare:** Software, Validation, Investigation, Writing – original draft, Writing – review & editing. **Umesh Chavan:** Conceptualization, Methodology, Formal analysis, Supervision, Software, Validation, Investigation, Writing – original draft, Writing – review & editing.

Data availability

Data will be made available on request.

Declaration of Competing Interest

The authors declare that they have no known competing financial interests or personal relationships that could have appeared to influence the work reported in this paper.

References

[1] Volodymyr Sirenko, Upendra S. Rohatgi, et al., Methods of Reducing Vehicle Aerodynamic Drag, BNNLL– 998083094-200-122-0C1P2 Puerto Rico, USA, 2012, pp. 8–12.

[2] M. Koike, Tsunehisa Nagayoshi, and etall, Research on Aerodynamic Drag Reduction by Vortex Generators, Mitsubishi Motors Tech. Rev. (2004).

[3] J. Singh, J.S. Randhawa, CFD Analysis of Aerodynamic Drag Reduction of Automobile Car - A Review, Int. J. Sci. Res. (2014).

[4] Bhavini Bijlani, Arvind S. Sorthiya, et al., Experimental and Computational Drag Analysis of Sedan and Square-Back Car, Int. J. Adv. Eng. Technol. (2013) 63–65.

[5] A. Parab, Ammar Sakarwala and etall, Aerodynamic Analysis of A Car Model Using Fluent- Ansys14.5, Int. J. Recent Technol. Mech. Electr. Eng. (2014) 7–13.

[6] D. Ramasamy, K. Kadirgama, A. K. Amirruddin, et al., Vehicle Body Drag Analysis Using Computational Fluid Dynamics, in: National Conference in Mechanical Engineering Research. ISBN: 978-967-5080-9501.

[7] R.B. Sharma, Ram Bansal, CFD Simulation for Flow over Passenger Car Using Tail Plates for Aerodynamic Drag Reduction, IOSR J. Mech. Civil Eng. (2013) 28–35.

[8] J. Singh, J.S. Randhawa, CFD Analysis of Aerodynamic Drag Reduction of Automobile Car -A Review, Int. J. Sci. Res. (2014).

[9] T. Engin, Halit Yaşar and etall, Design optimization of a shell-and-tube heat exchanger with novel three-zonal baffle by using CFD and taguchi method, Int. J. Therm. Sci. (2020).

[10] W.T. Cheng, H.C. Li, C.N. Huang, Simulation and optimization of silicon thermal CVD through CFD integrating Taguchi method, Chem. Eng. J. (2008) 603–613.

[11] J. Leuschen, K.R. Cooper, Full-Scale Wind Tunnel Tests of Production and Prototype, Second-Generation Aerodynamic Drag- Reducing Devices for Tractor-Trailers, SAE Int. (06CV-222) (2006).

[12] Ashfaque Ansari, Rana Manoj Mourya, Drag Force Analysis of Car by Using Low Speed Wind Tunnel, Int. J. Eng. Res. Rev. (2014) 144–149.

[13] S.A.C. Manaldesa, H.J. Nagarsheta, A Comparative Assessment of two Experimental Methods for Aerodynamic Performance Evaluation of a Car, J. Sci. Ind. Res. (2008) 518–522.

[14] S.C. Duve, M.K. Agrawal, An Experimental Study of Pressure Coefficient and Flow Using Sub Sonic Wind Tunnel The Case of A Circular Cylinder, Int. J. Emerg. Technol. Adv. Eng. (2014).